Check for updates

Densification mechanism of deep low-permeability sandstone reservoir in deltaic depositional setting and its implications for resource development: A case study of the Paleogene reservoirs in Gaoshangpu area of Nanpu sag, China

Shilin Wang[1], Xiran Yang[2], Yuanyuan Lu[3], Peidong Su[1]*, Dong Liu[4], Lingjian Meng[4], Qi Wang[4], Liang Li[4] and Ahmed E. Radwan[5]

[1]School of Geoscience and Technology, Southwest Petroleum University, Chengdu, China, [2]Exploration and Development Research Institute, PetroChina Southwest Oil & Gas Field Company, Chengdu, China, [3]CNOOC Research Institute Ltd., Beijing, China, [4]Exploration and Development Research Institute, Jidong Oilfield Company, PetroChina, Tangshan, Hebei, China, [5]Faculty of Geography and Geology, Institute of Geological Sciences, Jagiellonian University, Kraków, Poland

A better understanding of reservoir densification mechanisms is very important for petroleum exploration and controlling the reservoir quality distribution in low-permeability reservoirs. Low porosity and low permeability, difficult reconstruction, and economic infeasibility are important factors restricting its efficient production. Systematic analysis was performed to study the evolution of different microfacies in the deltaic depositional setting of the Paleogene deep low-permeability Gaoshangpu reservoir, define their genetic mechanisms, delineate the dominant facies belts, and define the favorable diagenetic sequences that are important for exploration of high-quality reservoirs. To understand the tight genesis of the low-permeability reservoirs, we analyzed the sedimentological and diagenetic evolution characteristics of various microfacies (i.e., underwater distributary channel, distributary bay, mouth bar, and front sheet sand) using core data and physical property analysis of the reservoir sand body. The results show the underwater distributary channel and estuary bar sand body with medium-to-fine-grained and poor−medium sorting. The diagenesis is dominated by strong compaction, calcareous, argillaceous cementation, and dissolution during stage B in early diagenesis and stage A in middle diagenesis. In the fan delta environment, the weak anti-compaction resistance of low-permeability reservoirs is mainly due to the large content of plastic particles, finer grain size, and medium−poor sorting, with an average porosity reduction rate of 65%. This is a key factor for densification of reservoirs above 3000 m. Comparison among different sandstone microfacies of the deltaic setting shows that the

sand body of the underwater distributary channel with low shale content has slightly stronger compaction resistance. The porosity reduction is not obvious at the depth of 3,000−4,000 m, but the loss of permeability at this depth section is significant, and the reservoir improvement from later dissolution is most obvious at this depth section. Calcareous cementation is the cause for densification of some mouth bars in the early stage and of underwater distributary channels in the middle and late stage. Under the influence of strong compaction and calcareous-filling pore throat, the sand body of the mouth bar has been basically densified at 3,000 m, resulting in limited reservoir transformation from later dissolution. The study shows that compaction is the main cause of reservoir densification, argillaceous and calcareous cementation is the secondary cause, and later dissolution is another main cause of reservoir enhancement. The research results can provide a reference and direction for reservoir development and search for the high-quality sweet spot in the deep and low-permeability reservoir.

1 Introduction

Low-permeability sandstone reservoirs or tight reservoirs are one of the most important hydrocarbon resources worldwide (Law and Dicknson, 1985; Karim et al., 2010; Zou et al., 2012; Li et al., 2019a). Many researchers have investigated low-permeability reservoirs in terms of sedimentological, diagenesis, and petrophysical properties (i.e., porosity and permeability) for better control of these important reservoirs (Xi et al., 2015; Yang et al., 2016a; Lai et al., 2016; Li et al., 2021a). Typically, low-permeability sandstone reservoir productivity could be dependent on primary sedimentation conditions or secondary diagenetic and fractured types, as well as the development of enigmatic sweet spots or the basin petroleum system (Shanley et al., 2004; Zeng et al., 2010; Li et al., 2018a). Such low-permeability reservoirs have unique petrophysical and sedimentological characteristics that need to be fully understood to mitigate misunderstanding of these attributes and wrong subsurface interpretation. For example, identifying the densification mechanism in low-permeability reservoirs and the match between the pore evolution history and the hydrocarbon generation time is of interest to researchers in critical resource assessment (Bjørlykke, 2014). Diagenesis is the most effective reservoir control method for forming the current reservoir conditions (Xi et al., 2015). To predict the reservoir performance and define the formation mechanism of these low-permeability reservoirs, a comprehensive knowledge of the relationships between depositional fabric, routine vs. effective permeability, and pore geometry under the conditions of overburden stress is a fundamental request according to Shanley et al., 2004; Wang et al., 2013; Mingjie et al., 2014; Xi et al., 2015; Ren et al., 2019. The deep low-permeability reservoirs are expected to have more complex depositional and diagenetic features that impact the quality of these reservoirs. However, few studies have been directed toward the deep low-permeability reservoirs in different depositional settings and different microfacies, which remain scarce. Therefore, the example of the Paleogene deep low-permeability reservoir from the Gaoshangpu oilfield, Nanpu Sag, China was examined in this work.

The Gaoshangpu area is a main oil-producing area with high and stable production in Nanpu Sag and also an oil-rich depression in the Bohai Bay Basin. The Paleogene Submember 2 + 3 substratum in Section 3 of the Shahejie Formation (Es_3^{2+3}) is the main oil-bearing series in the Gaoshangpu oilfield (Liu et al., 2022), in which the low-permeability reserves account for more than 80% of the undeveloped reserves in the Jidong oilfield. With the deepening of exploration, the proportion of low-permeability reserves of undeveloped reserves in the Jidong oilfield is increasing, which has potential as an important strategic resource for stable production in the future. The buried depth of the low-permeability reservoir is 3,000–4100 m, with the oil-bearing interval having a depth of 600–700 m (Xu et al., 2020), and the production at different depths and blocks varies greatly. There are both conventional reservoirs and difficult-to-recover low-permeability reserves. The proven oil-bearing area of Es_3 is 17.4 km^2, and the proven geological reserves are 38.02 million tons, while daily oil production is about 251 tons, that is to say, the oil recovery rate is only 0.32%. Reservoir heterogeneity is strong, and physical property span is large with a porosity of 6%–24% and permeability of 0.5~100 $\mu m^2 \times 10^{-3}$ μm^2 (Liu et al., 2022; Yang et al., 2016b; Xie et al., 2017; Lai et al., 2018). The low-permeability reserves in deep Gaoshangpu reservoirs account for a large proportion of undeveloped reserves in the Jidong oilfield. The reasons for its inefficient exploitation include its tight and low-permeability features, as well as its hard-to-transform and

FIGURE 1
Structure location and well location map of the Gaoshangpu oilfield.
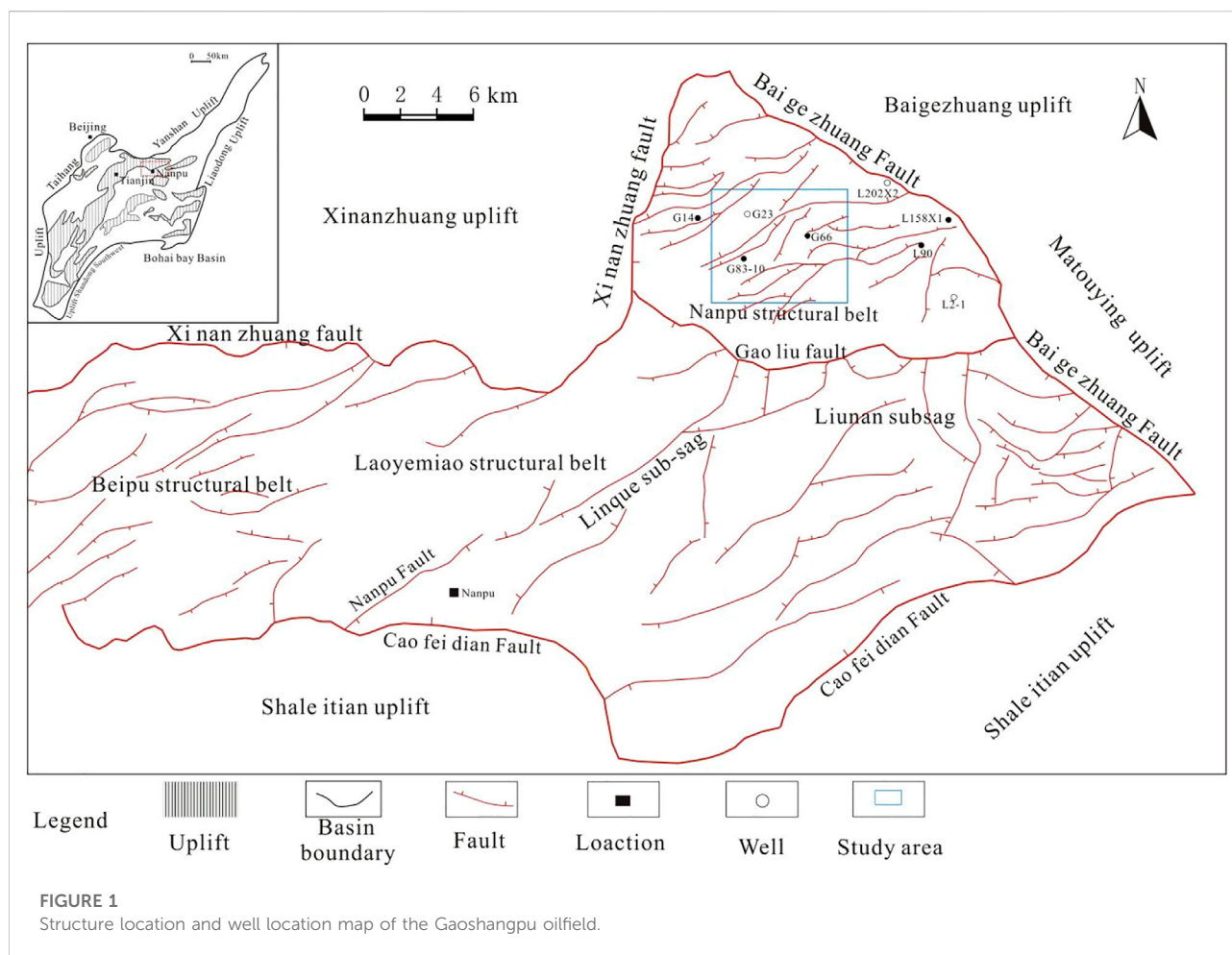
economically unfavorable nature. The evaluation and study of the deep low-permeability reservoir in Gaoshangpu is of great significance for the subsequent development policy and its efficient development. A great deal of study has been carried out on sedimentary characteristics, diagenetic evolution, heterogeneity, time-varying characteristics, sensitivity, etc. (Gao et al., 2016; Li et al., 2018b). The possibility and favorable controlling factors of the high-quality reservoirs in the middle and deep layers of Nanpu Sag are discussed in detail, which not only enhances the confidence in the exploration and development of deep oil and gas resources but also points out the direction for efficient exploration and development of high-quality reserves in the middle and deep layers. However, the difference in diagenetic evolution of different micro-facies reservoir sand bodies, the tight genetic mechanism of low-permeability reservoirs, and the diagenetic evolution of dominant reservoir facies sand bodies still need to be studied in depth. Also, it is the key factor in determining favorable sedimentary and diagenetic facies belts and predicting favorable desert areas. Based on the theories of sedimentology, reservoir geology, and development geology, the authors carried out the

research through the data of core observation, thin section identification, scanning electron microscope, X-ray diffraction, and physical property analysis.

Through systematic analysis of the formation and evolution of different micro-facies reservoirs in the fan delta, the genetic mechanism of low-permeability reservoir and the dominant facies belts and favorable diagenetic sequences are defined, and meanwhile, the possibility of high-quality reservoirs formed in deep low-permeability reservoirs is further explored. It provides a geological basis for oilfield increase in reserves and production, as well as for efficient development of the Gaoshangpu reservoir, and meanwhile, it provides a reference for evaluation of other low-permeability reservoirs in Nanpu Sag and similar areas that have the same geological conditions.

2 Geological setting

Gaoshangpu oilfield is located in the northern part of Nanpu Sag and the eastern part of the structural belt next to

FIGURE 2
Sedimentary facies diagram of the Gaoshangpu Oilfield.
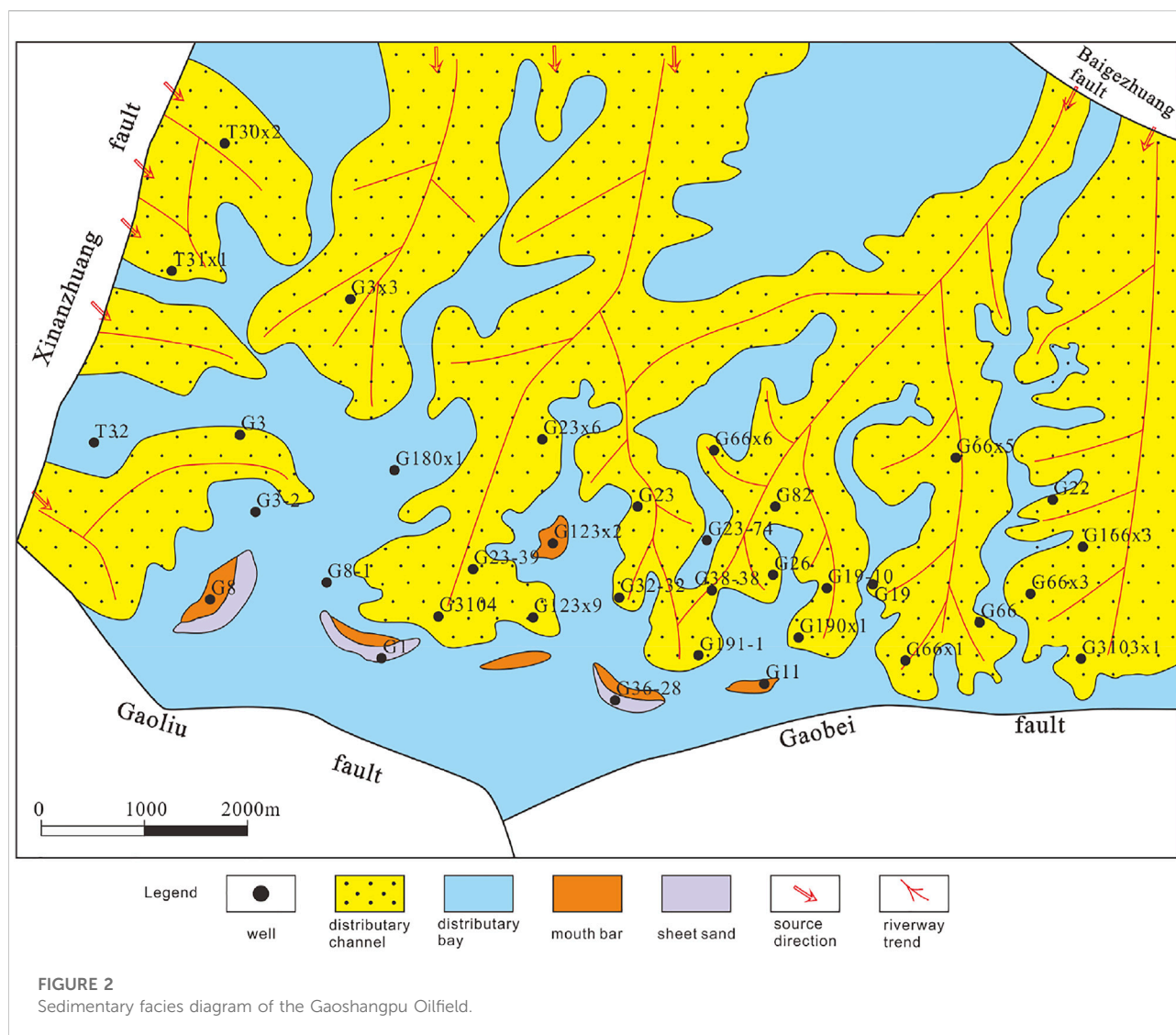
Liuzan oilfield. The northern part of the oilfield is sandwiched by the Xinanzhuang and Baigezhuang faults (Figure 1). It is an anticline structure complicated by faults. The main structure covers an area of about 20 km² with developed faults and broken fault blocks. The deep low-permeability Gaoshangpu reservoir, which is NW-trending, is located on the upthrown side of the Gaoliu fault in the steep slope zone of the Nanpu Sag. It is cut into several fault blocks by NW-trending, NE-trending, and nearly EW-trending faults. The Quaternary Pingyuan Formation (Q), Neogene Minghuazhen Formation (Nm), Guantao Formation (Ng), Paleogene Dongying Formation (Ed), and Shahejie Formation (Es) are developed from top to bottom in the Gaoshangpu oilfield. The Shahejie Formation can be further divided into Es_1, Es_2, and Es_3. There are five sets of marker beds in the whole formation. The largest marker bed in this area is the mudstone section of the oil group 0 in sub-member of Es_3.

Es_3 was in the developing stage in the fault basin. A set of fan delta sedimentary bodies deposited rapidly near the source and steep bank with strong alluvial capacity, and the provenance lies in the north and NE. Two subfacies developed, namely, fan delta front and pro-fan delta, of which the fan delta front can be divided into four microfacies as the underwater distributary channel, distributary bay, mouth bar, and front sheet sand, and the pro-fan delta mainly develops far sand bars (Figure 2). The sediments are dominated by lithic feldspar sandstone, with low component maturity and structural maturity. The sand body of an underwater distributary channel is characterized as fining upward, and the erosion surface can be seen in some locations. The natural gamma curve is box-shaped or bell-shaped. The sand body of the mouth bar is characterized as coarsening upward, with obvious cross bedding on the top and a funnel-shaped natural gamma curve.

3 Samples and methods

3.1 Samples

In this study, the experimental samples came from the sandstone of the third member of the Gaoshangpu Oilfield. In order to analyze the difference in the storage performance of the reservoir rock under different depositional environments and depth conditions, targeted sampling of reservoirs is carried out in different depositional environments, and the sampling depth is between 3,200 and 4300 m.

3.2 Experimental methods

3.2.1 Porosity and permeability test

The porosity and permeability tests of samples adopt the AP-608 overburden porosity-permeability tester. Before the experiment, the sandstone sample is made into a cylindrical shape of 1 cm × 3 cm (diameter × length), and the cylindrical sample is placed in the experiment process. In the Hassler core holder, the porosity and permeability tests are automatically measured by the instrument. The permeability is obtained by the non-steady state pulse attenuation, and the porosity test passes the Boyle's law test.

3.2.2 Storage space type

The observation of the storage space type adopts the casting thin section and scanning electron microscope. The casting thin section is made by the ZT-2 rock casting instrument. The samples will be evacuated during the production process. The casting body is made of colored epoxy resin. The observation of the type of thin pore space is carried out with an XP607 polarizing microscope.

The scanning electron microscope test uses a Quanta 450 environmental scanning electron microscope produced by FBI Company to observe the microscopic pore structure of shale. Before the experiment, the sample is cut into dimensions of 5 mm × 5 mm × 3 mm, and the surface of the experimental sample is polished with argon ions. At the same time, an ion mill is used to show and grind the sample to eliminate surface irregularities. The processed sample is placed on the sample table, and SEM is used to observe the type of pores on the polished surface.

3.2.3 Pore structure

The pore structure of the sample was obtained by a high-pressure mercury intrusion experiment PoreMaster60 automatic mercury intrusion instrument produced by the United States Conta Company. Before the experiment, the sample was made into a 2.5 cm × 3.5 cm (diameter × length) standard core. The test process was carried out in a well-ventilated, room-temperature environment. The experiment process adopted continuous
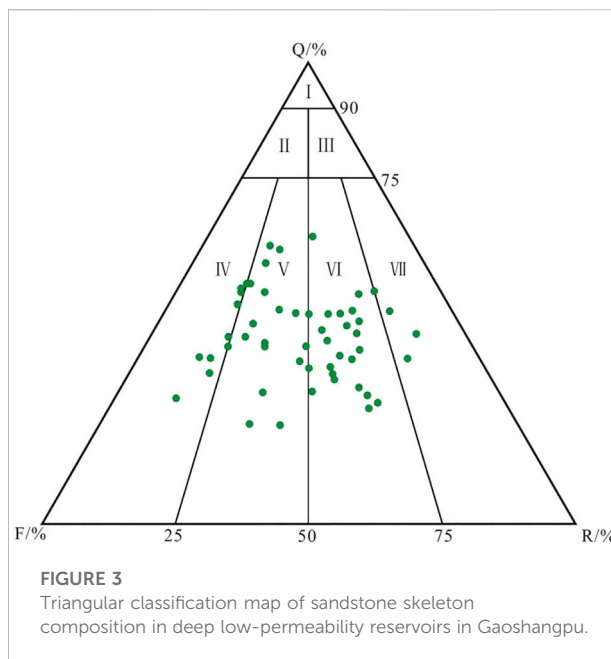

FIGURE 3
Triangular classification map of sandstone skeleton composition in deep low-permeability reservoirs in Gaoshangpu.

pressure, and the pore median radius was automatically calculated by the instrument.

4 Results and discussion

4.1 Reservoir characteristics

4.1.1 Sedimentology characteristics

Es_3 is a set of fan delta sedimentary products, close to the provenance. Several types of sedimentary microfacies, such as underwater distributary channels, mouth bars, sheet sands, interdistributary bays, and distal bars, are developed. The sand bodies developed under different sedimentary microfacies have huge differences in scale and reservoir effectiveness. For the study area, the effective reservoir is mainly composed of an underwater distributary channel and mouth bar (Wang et al., 2010; Wang et al., 2013). The shale content in underwater distributary channels and mouth bars is low, with coarser grain sizes and larger-scale sand bodies. However, sheet sand, interdistributary bay, and distal bar mainly consist of argillaceous siltstone, siltstone, and mudstone with relatively small sand body scale. Therefore, the following mainly introduces the underwater distributary channel and mouth bar.

4.1.2 Lithological characteristics

Deep low-permeability Gaoshangpu reservoirs are dominated by medium and fine sandstones, with 67%–91% rigid grain composition and an average ratio of about 81.4%. The contents of cuttings, feldspar, and quartz are roughly the same, mostly feldspar sandstone and feldspar lithic sandstone

FIGURE 4
Histogram of physical property distribution of high-depth and low-permeability reservoirs.
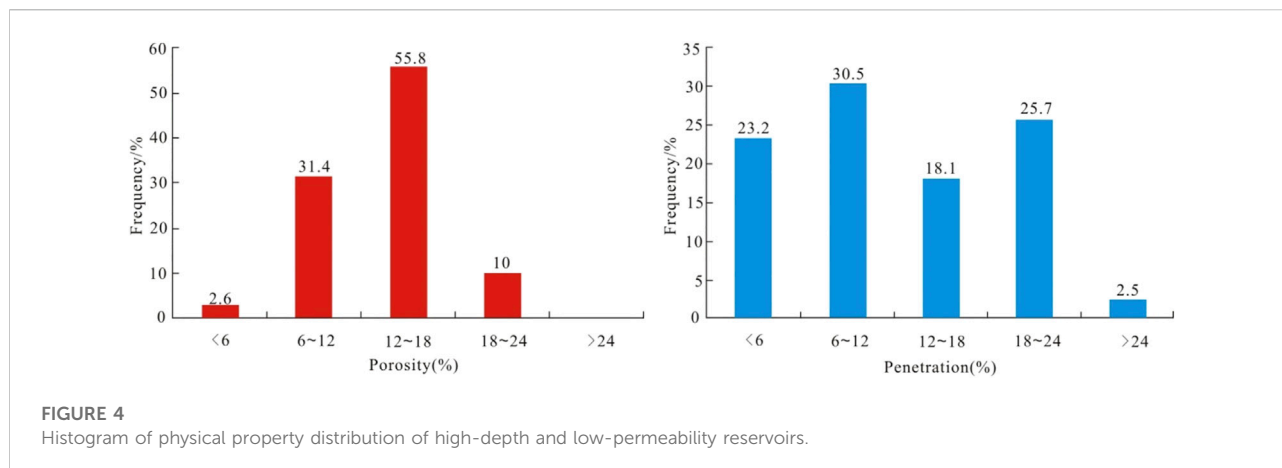
([Figure 3]). The cement is mainly argillaceous and calcareous, as well as quartz overgrowth. The argillaceous content is 2%–19%, with an average of about 8.4%. The average content of cement is 5.6%, and the main types of cement are porous cementation and line contact cement. The clay minerals are mainly composed of illite–montmorillonite mixed layer and chlorite. The detrital sediments are characterized by strong erosion, rapid transportation, and rapid accumulation (Fan et al., 2020b; Fan et al., 2020c).

The sand skeleton particles in the underwater distributary channel are poor–medium sorted with the sorting coefficient ranging between 1.41 and 2.17. The roundness is medium, the particle size lies between 0.18 and 0.59 mm, and the shale content is generally less than 7%. The mouth bar is characterized as inverse grading. The lithology is mainly fine sandstone and medium sandstone, with the sorting coefficient between 1.23 and 1.45. The roundness is good, with the particle size lying between 0.15 and 0.32 mm. Argillaceous content is slightly higher, ranging from 5% to 10%. The sediments in the distal bar are relatively fine, which are deposited in the process of the sand body being pushed to the lake, developing into a transitional relationship with the pre-delta mudstone, where very few thin coarse sand layers can be seen. The sorting coefficient is between 1.9 and 4.2. Sand body roundness is medium–good, with the particle size between 0.02 and 0.13 mm. The shale content is generally greater than 10%. The sediments of the sheet sand and the mouth bar are similar. The differences lie in the shape of the sand body and the amount of shale content. The shale content of sheet sand is slightly higher, which is mainly reflected in argillaceous lamina, silty mudstone, and mudstone interbedded development.

4.1.3 Physical characteristics

According to the analysis results of the rock porosity test, the porosity of the deep low-permeability Gaoshangpu reservoir is mainly distributed between 6%–20%, accounting for 80%

porosity, with the average porosity being 14.3%. The reservoir permeability is mainly distributed in $1 \mu m^2 \times 10^{-3} \mu m^2$–$10 \mu m^2 \times 10^{-3} \mu m^2$ and $20 \mu m^2 \times 10^{-3} \mu m^2$–$50 \mu m^2 \times 10^{-3} \mu m^2$, and the average permeability is $9.98 \mu m^2 \times 10^{-3} \mu m^2$. According to the classification standard of reservoir porosity in the petroleum industry (ST/T 6285-1997), the reservoir is a low-permeability to ultra-low-permeability reservoir ([Figure 4]). The physical properties of the underwater distributary channel and mouth bar are the best. The average porosity is 18.5% and 15.1%, respectively, and the average permeability is $17.8 \mu m^2 \times 10^{-3} \mu m^2$ and $12.5 \mu m^2 \times 10^{-3} \mu m^2$, respectively. The porosity and permeability of the interdistributary bay sand bodies have no obvious changes in different diagenetic stages, and the porosity is between 5% and 15%, and the permeability is between $0.01 \mu m^2 \times 10^{-3} \mu m^2$ and $0.5 \mu m^2 \times 10^{-3} \mu m^2$. The porosity and permeability of the far-bar sand bodies decrease with the deepening of the diagenetic stage. The porosity is between 5% and 20%, and the permeability is between $0.01 \mu m^2 \times 10^{-3} \mu m^2$ and $0.5 \mu m^2 \times 10^{-3} \mu m^2$. The porosity and permeability of the sheet sand reservoir have obvious differences at different depths. The porosity is between 5% and 15%, and the permeability is between $0.01 \mu m^2 \times 10^{-3} \mu m^2$ and $5 \mu m^2 \times 10^{-3} \mu m^2$.

4.1.4 Reservoir space types and characteristics

According to the observation results of the scanning electron microscope and microsection, the pore types of the reservoir include primary residual pore, intergranular solution pore, intragranular dissolved pore, mold pore, and other clay micropores ([Figure 5]). Intergranular and intergranular dissolution pores are well-developed ([Figures 5A,E,F]), accounting for 8%–90% and 5%–15%, respectively, and primary residual intergranular pores accounted for 3%–32.6%. The selective dissolution leads to uneven distribution of dissolved pores between and within grains, resulting in further enhancement of reservoir heterogeneity,
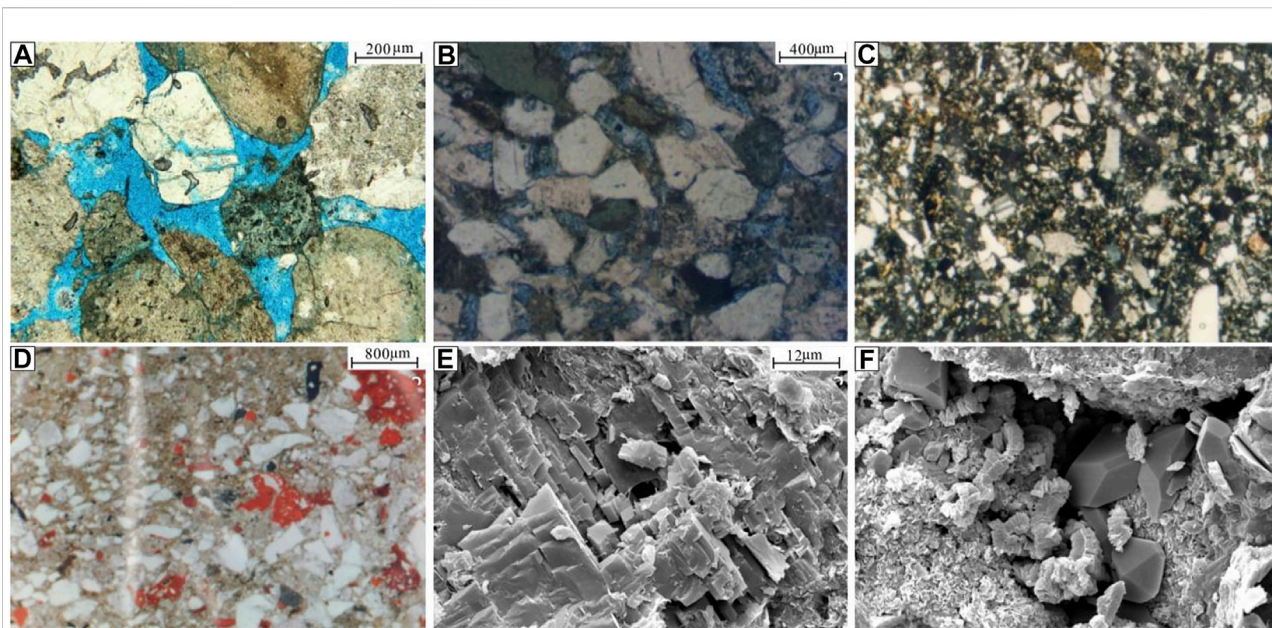
FIGURE 5
(A). Reservoir space types of the high-deep reservoir of the third member of Shahejie Formation in Gaoshangpu oilfield, Nanpu Sag. **(A)**. GJ3102-8, 3,131.24 m, gravel-bearing medium sandstone in the underwater distributary channel, with developed primary pores and a small amount of intergranular and intragranular dissolution pores, and the throats are flaky and bundled throats; **(B)**. G32-30, 3,476.1 m, distributary estuary bar fine sandstone, dissolution pores, mold holes, throats are mainly bundled, and fine throats; **(C)**. G58-33, 3629 m, sheet sand argillaceous fine siltstone, few remaining primary pores, mainly micropores, and intragranular dissolved pores in the clay, and fine throats as the main throat; **(D)**. G83-10,3663.8 m, far sand bar argillaceous fine siltstone, basic pores are basically not developed, a few secondary dissolved pores are developed, there are more clay micropores, poor pore permeability, and fine throat mainly; **(E)**. GJ5-44, 3169 m, intragranular dissolution pores of feldspar; **(F)**. GJ5-44, 3,164.8 m, remaining intergranular pores.

complicated pore throat structure, and poorer pore connectivity (Figure 5).

There are several types of pore throat structures, such as medium pore with medium–fine throat type, medium–fine pore with fine throat type, fine pore with fine throat type, and micropore with micro-throat type (Figure 5). Throat types are mainly necking, schistose, or micro-throats with poor connectivity (Figures 5B–D). The high-value range of the throat width is 15.38–62.32 μm and the low value range is 1.27–2.98 μm, with an average throat width between 5.73 and 19.97 μm. The coordination number indicates the number of throats connecting the pores. The maximum coordination number is 1–5, and the average coordination number is 0.02–0.42, which determines that it is a coarse throat with a low coordination number, and the pore connectivity is medium to poor.

4.2 Characteristics and evolution sequence of diagenesis

4.2.1 Features of diagenesis

The Es3 Formation in the Gaoshangbao oilfield is buried below 4000 m, and the diagenesis is complex (Figure 6). Based on

the relationship between physical property and depth and the relationship between the initial porosity and the separation coefficient proposed by Lundegard, the primary porosity of the surface of the subaqueous distributary channel reservoir is estimated to be 37%–45%. The initial porosity of the mouth bar is 39%–55%. The overall compaction rate of the deep low-permeability Gaoshangpu reservoir is 66.3%, which shows medium–strong compaction. The cementation is dominated by carbonate minerals and argillaceous cementation, with a small amount of kaolinite and siliceous cementation filling and feldspar dissolution, which account for 7.5% of the secondary pores in the study area. The characteristics of reservoir diagenesis of different sedimentary microfacies are studied. The results show that the overall compaction of the underwater distributary channel is weak, and the particles are mainly in point or line contact. The content of shale is relatively small, and the cementation is mainly siliceous and calcareous cementation. The secondary growth of quartz can be enlarged to grades II–III. The authigenic microcrystalline quartz can also be seen (Figure 5E). The average content of quartz cement is 2.0%. Most corrosions are feldspar dissolution, and a small amount of corrosions are debris dissolution. The compaction is gradually enhanced in the middle and late stages of diagenesis with strong calcareous cementation (Li et al., 2019c; Li et al., 2020; Li et al.,

FIGURE 6
Burial history of Es$_3^{2+3}$ in well G87 in the Gaoshangpu oilfield.
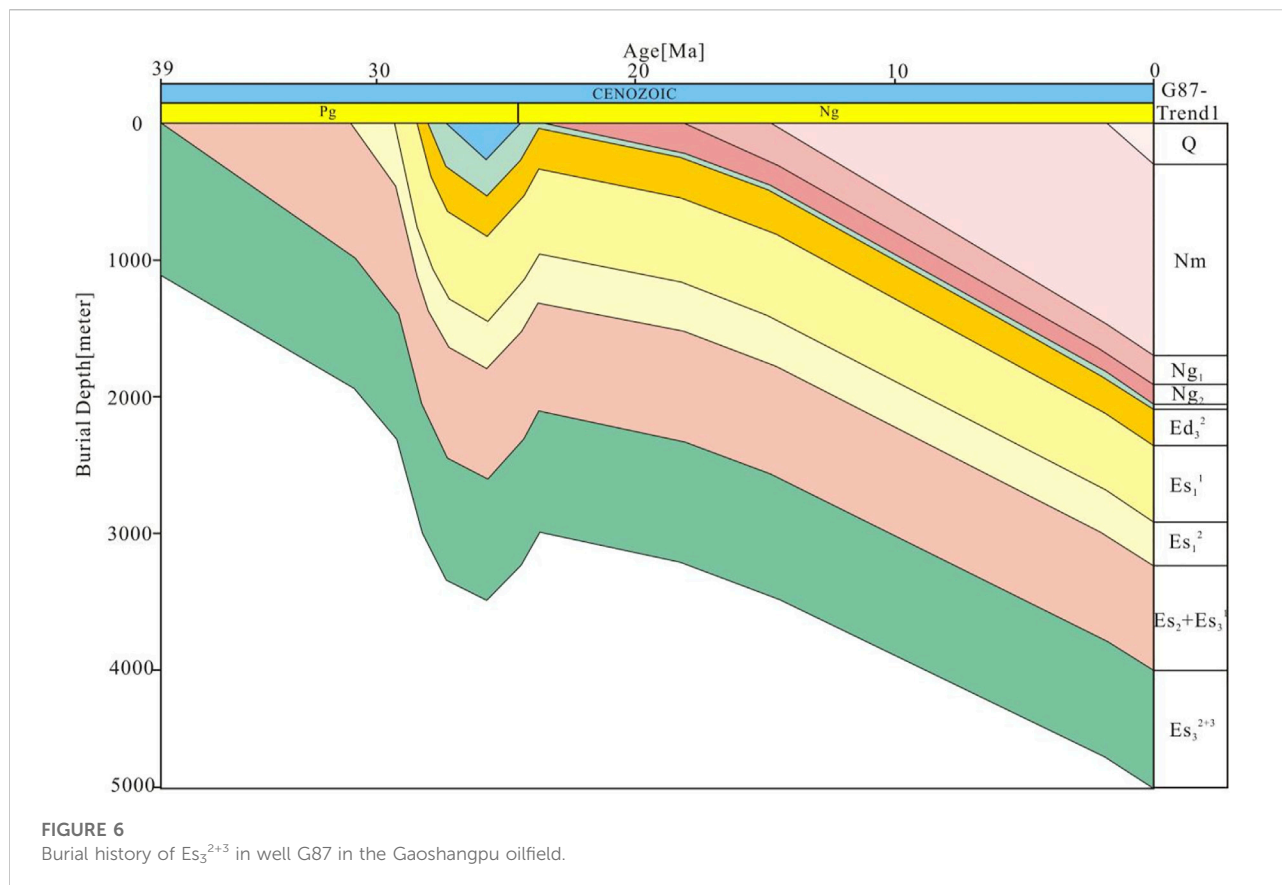
2021b; Li, 2022). The primary intergranular pores and solution pores are developed in the early stages, and the solution pores are dominant in the middle and late stages.

The reservoir sand body of the mouth bar was initially compacted above 3000 m, and then the reservoir was further densified by mechanical compaction. The diagenesis is mainly calcareous cementation and strong compaction. The average content of calcite is 5%, and the highest value can reach 14%. Calcite replacing feldspar could be seen, and the dissolution is weak. The silicon content increased, and calcareous cementation is obviously enhanced. Calcite–crystal cementation can be seen locally, showing a calcium tip on the curve. Intergranular pores are commonly found as residual intergranular micropores and dissolved pores, which come from feldspar and debris dissolution. The distal bar, sheet sand, and interdistributary bay have higher plastic mineral content. After strong mechanical compaction and calcareous cementation above 3000 m, a few intergranular pores with weak siliceous cementation and dissolution remain. Dissolution mostly occurs in feldspar and lithic minerals along fractures or bedding (Li et al., 2019b; Fan et al., 2020a; He et al., 2020; He et al., 2021; He et al., 2022a; Li et al., 2022a; Li et al., 2022b; Fan et al., 2022).

4.2.2 Diagenetic stages

Deep low-permeability Gaoshangpu reservoirs have been subjected to diagenesis, such as strong compaction, cementation, and dissolution (Guo et al., 2019). Sampling distraction in the study area showed that the reflectance of vitrinite ranged from 0.5% to 0.9% and the ratio of the illite/smectite interlayer from 25% to 70%, with an average of 55%. Primary pores and secondary pores are well-developed. Primary pores are mainly developed in the middle and lower parts of the layers, and secondary pores are concentrated in the lower part of the reservoir. According to the classification criteria for diagenetic stages of clastic rocks (ST/T5477—2003), the diagenetic stage in the studied reservoirs is between early diagenetic stage B and middle diagenetic stage A (Figure 7).

4.2.3 Diagenetic sequence

Diagenesis is an important factor affecting reservoir quality. Reservoir types with different pore structures and physical properties result from distinct diagenetic sequences, diagenetic stages, and diagenetic evolution (Zhu et al., 2009; He et al., 2022b; Wang et al., 2022). Based on the assemblage of diagenetic minerals of deep low-permeability Gaoshangpu reservoirs, it
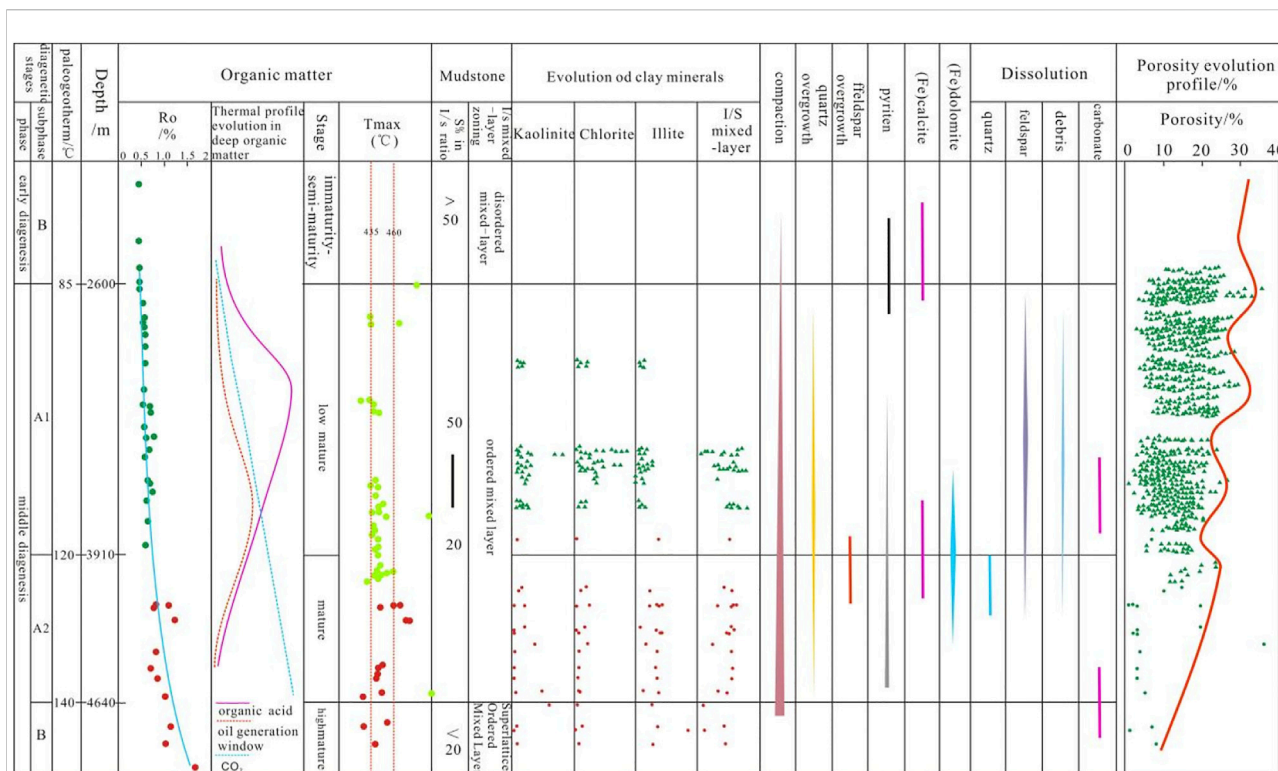
FIGURE 7
Division of diagenetic stages of the Gaoshangpu oilfield (modified by Jidong oilfield exploration and development research institute).

can be preliminarily determined that the sequence of diagenetic minerals or diagenesis is as follows:

Microcalcite-silica I stage overgrowth-weak dissolution of feldspar, debris-silica II stage overgrowth-kaolinite precipitation-large-scale feldspar, and lithic dissolution-silica III stage overgrowth-intergranular pores filled with quartz-(iron-bearing) calcite filling-dolosparite-weak dissolution.
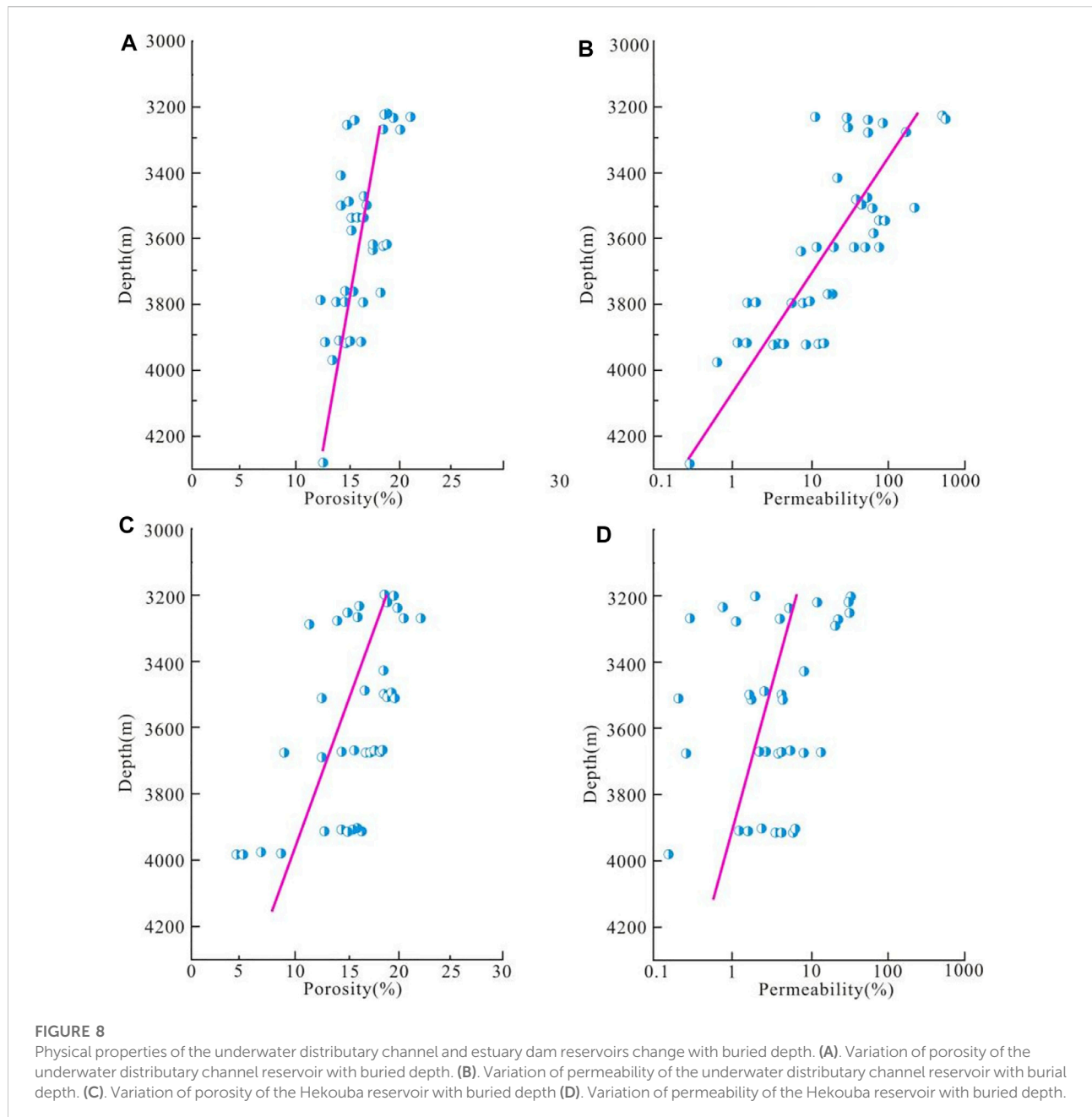
4.3 Influencing factors of low-permeability reservoir

4.3.1 Influence of sedimentary environment and sediment composition on reservoir

Due to the difference in hydrodynamic conditions and transport distances in each sedimentary environment, skeleton composition, grain structure, and impurity content of different microfacies sand bodies have different characteristics, which also have a profound influence on the evolution sequence and degree of burial diagenesis (Jiang et al., 2004; Li et al., 2010). With the increase in shale content and the decrease of average grain size, the diagenetic compaction becomes more intense (Wu et al., 2020; ZinsaloJoël et al., 2021). The physical properties of the distributary channel,

mouth bar, distal bar, and sheet sand reservoir at the same buried depth become worse successively. Due to the strong hydrodynamic conditions, the coarse sediment particles, slightly low content of miscellaneous base, and burial depth above 3500 m, the physical properties of the underwater distributary channel and distributary mouth sand bar are far better than those of the far sand bar and sheet sand. Among them, the underwater distributary channel is the best, and the permeability is nearly 10 times higher than that of the sand body of the mouth bar. Some far sand bars, sheet sand, beach bars, and thin sand layers in bay sand sheets buried more than 3000 m deep have already been densified.

When the buried depth exceeds 3000 m, the pore reduction of the underwater distributary channel is not obvious. However, the permeability decreases more significantly, while the situation of the sand body of the mouth bar is the opposite. Affected by water erosion, the energy of the water body of the underwater distributary channel is stronger when deposited; the mud content is lower than that of the mouth bar, and the pore is less affected by compaction. After the burial depth exceeds 3000 m, the overburden pressure of the skeleton particles increases and the porosity decreases only a little, but the contact between particles changes gradually from point contact to line contact, and thus the

FIGURE 8
Physical properties of the underwater distributary channel and estuary dam reservoirs change with buried depth. **(A)**. Variation of porosity of the underwater distributary channel reservoir with buried depth. **(B)**. Variation of permeability of the underwater distributary channel reservoir with burial depth. **(C)**. Variation of porosity of the Hekouba reservoir with buried depth **(D)**. Variation of permeability of the Hekouba reservoir with buried depth.

throat radius is significantly reduced (Figure 8). Therefore, the permeability loss is more than that of the estuary bar, but the porosity loss of the estuary sand bar reservoir with finer grain size and more plastic content is more obvious. With the intensity of compaction, the pore throat size decreases significantly, leading to reservoir densification in the underwater distributary channel. The particle size and shale content not only determine the intensity of compaction in the early stage and fluid activity in the later stage of the reservoir but also the intensity of later corrosion and cementation.

4.3.2 Effect of compaction on reservoir densification

The mechanical compaction becomes stronger with the increase in the buried depth of the reservoir. Low-permeability Gaoshangpu reservoir is deeply buried, whose main diagenesis are compaction and pressure dissolution (Gao et al., 2016). Under the same material condition, the pore structures of reservoirs at different depths are compared. The result shows that with the increase of burial depth, the radius of the pore throat decreases in multiples, and the permeability

FIGURE 9
Microscopic characteristics of underwater distributary channel reservoirs at different depths and corresponding mercury intrusion characteristics. **(A)** a$_1$. G65-1, 3225 m, median particle size 0.32 mm, mud content 3%, sorting coefficient 1.76, pore throat radius: 3.73 μm; **(B)** b$_1$. G62-35, 3602 m, median particle size 0.3 mm, mud content 2%, sorting coefficient 1.85, pore throat radius: 1.48 μm; **(C)** c$_1$. G66X5, 4285 m, median particle size 0.34 mm, mud content 2%, sorting coefficient 1.68, pore throat radius: 0.4 μm.

FIGURE 10
Relationship between carbonate content and physical properties of reservoir sand bodies in estuary bars and underwater distributary channels. **(A)**. Relationship between porosity and carbonate content; **(B)**. Relationship between permeability and carbonate content.

decreases exponentially. The original porosity of deep low-permeability Gaoshangpu reservoirs is 42%, and the porosity could be reduced to 17.26%–28.24% due to the compaction, with an average value of 20.8%. The compaction above 3800 m is generally less than 75% (Figures 9A,B), which is medium–strong compaction, while it could reach more than 75% below 3800 m, which is strong compaction. The average porosity below 3500 m in the study area is 15.5%, and the porosity reduction rate due to compaction is 65% (Figure 9C), which is medium–strong compaction. The proportion of reservoir porosity damaged by compaction increases gradually from the underwater distributary channel, mouth bar, far sand bar, and sheet sand. The underwater distributary channel sand bodies with coarse grain size, high maturity of grain structure, and low content of impurities have stronger compaction resistance, and the damage of porosity reduction by compaction is weak (Figure 9).

4.3.3 The differential effect of cementation on reservoir

Cementation is another main cause of reservoir densification. The degrees of cementation vary dramatically among low-permeability reservoirs of different microfacies. When the carbonate content exceeds 4%, the physical properties of the underwater distributary channel and mouth bar sand bodies show a significant decrease (Figure 10), with porosity basically less than 13% and the permeability less than $1\ \mu m^2 \times 10^{-3}\ \mu m^2$. There are two explanations for it. On the one hand, the carbonate cementation of sand bodies at the edge of channel sand bodies or toward the lake, as well as the sand bodies developed in thin interbeds of sand and mud, is stronger. The porosity loss of the distal bar reservoir due to cementation is significantly higher than that of the estuary sand dam. On the other hand, during the cementation development, underwater distributary channels are deposited earlier than the mouth bar and distal bar sand bodies, with better preservation of intergranular pores and relatively undeveloped early calcium cementation. The components of early calcareous and argillaceous cement increased gradually in the mouth bar and distal sand bar reservoirs. While the primary intergranular pores and throat were poorly preserved, and the late calcareous cementation has an obvious influence on the underwater distributary channel reservoir with relatively well-preserved pores.

4.3.4 The effect of dissolution on reservoir

Dissolution is a commonly developed diagenesis in reservoirs in the study area, which plays an important role in improving the quality of reservoirs in the middle and late stages and is also the main reason for development of high-quality reservoirs (Wang et al., 2010; Lan et al., 2014; Wang and Chen, 2016; Li et al., 2018c; Li et al., 2022c). The organic acid released during the maturation of organic matter dissolves the feldspar particles in the reservoir. Affected by diageneses such as compaction and cementation of early diagenesis, the physical properties of the

reservoir were damaged to some extent, and the effect of dissolution on the densified reservoir is limited. For underwater distributary channel reservoirs with good original properties, the cumulative porosity damage of compaction and cementation averages to about 50%. After compaction, the porosity of the mouth bar reservoir is damaged by more than 60% on average, and the fluid activity is restricted seriously in the later stage. The occurrence of reservoir dissolution is directly related to the activity of formation water. Among the underwater distributary channel sand bodies, feldspar has suffered strong dissolution, followed by mouth bar sand bodies. The physical properties of reservoirs in these genetic types of sand bodies may be improved obviously. Microscopic thin-section analysis shows that the content of feldspar-dissolved pores in low-permeability reservoirs is less than 5%, indicating that the lack of dissolution in low-permeability reservoirs is another important reason for reservoir compactness. After the dissolution of different microfacies reservoirs, the difference in reservoir quality is further increased.

4.4 Densification mechanism of deep low-permeability Gaoshangpu reservoir

By comparing different microfacies reservoirs with the same burial depth, it can be seen that after the early diagenetic evolution, reservoir sandbodies of different grain sizes, sorting, and shale contents have distinct characteristics at the depth of 3,000–3500 m (Figure 5). In the process of diagenetic evolution, the underwater distributary channel reservoirs with coarse grain size, less shale content, and better sorting preserved better primary intergranular pores (Figure 5A). Primary pores could be preserved at this depth, and dissolution pores and primary pores are developed in this section, which are favorable for dissolution of the reservoir as acid fluids carried by the expulsion process can enter the reservoir during the late formation water activity. The grain size of the reservoir sand body in the mouth bar is slightly finer, and the clay content is slightly larger (Figure 5B). Therefore, during the early stage of mechanical compaction, a large number of plastic particles in the reservoir have been adjusted by compaction, arranged in layers, accelerated by pressure solution, and so on, and therefore the porosity has been significantly reduced. The porosity of this depth interval is 5%–10% less than that of the subaqueous distributary channel reservoir sand body, and the permeability is about 10 mD–200 mD less. Most of the sandbodies in the interdistributary bay, distal bar, and sheet sand above 3000 m have been densified (Figures 5C,D). The reservoir is of low permeability and ultra-low-permeability with a porosity of only 5%–15%, permeability less than 10 mD, and a pore throat radius less than 0.2 μm. In the later stage, the fluid percolation capacity is poor and the dissolution

transformation is not obvious. The early densification of reservoirs results from strong compaction and pressure dissolution in the early stage with a high content of plastic particles and weak calcareous cementation in the early diagenetic stage. The reservoirs formed with different sedimentary microfacies above 3000 m are characterized by different grain sizes, shale content, and sorting, which are the main factors affecting the reservoir densification.

The mouth bar sand bodies penetrate into the lake, and the dissolved calcium in the river gradually precipitates out in the sediment. Calcareous cementation was developed in the early diagenetic stage, and hence a large amount of calcite with crystal cementation resulted in densification of the reservoir. In the later period, only a few particle components were dissolved by fluid activity, and some micropores and intergranular pores were formed. If the dissolution lasts for a long time, casting pores can be formed. Among some mouth bar sandbodies with a slightly higher clay content, calcareous cementation is generally not developed. In the process of diagenetic evolution, the compaction resistance of the reservoir is poor, so the reservoir section has been densified at this depth. High shale content, fine grain size, and calcareous cementation are the main reasons for low permeability and densification of the mouth bar reservoir. Its degree of corrosion is relatively less obvious than that of the underwater distributary channel sand body. The plastic particle content of distal bar and sheet sand is very high, and the compressive strength is weak. A large number of primary pores have been lost during the early diagenetic stage A. After the early diagenetic stage, argillaceous cementation and a small amount of calcareous cementation have filled up most of the primary pores. The porosity is only about 10%, and the permeability is as low as 0.5 mD–10 mD at a depth of 3,000–3500 m, which indicates that the early diagenetic stage has resulted in severe densification of these micro-facies reservoirs. Strong compaction is an important reason for reservoir compaction.

Volume fracturing is conducted to communicate some dead pores because of the underwater distributary channel with undeveloped calcareous cementation and parts of the reservoir sand body with decreased permeability of the mouth bar. The connectivity between pores and sand bodies ensures efficient production of such reservoirs. For low-permeability reservoirs with calcareous development, acidizing and fracturing could be used to improve connectivity and increase production.

In the sedimentary environment of fan delta, the fast accumulation of sediments, low degree of sorting and grinding, and relatively high content of mud and plastic particles, such as debris particles, lead to weak compaction resistance of reservoirs, which is the main reason for strong compaction of deep low-permeability Gaoshangpu reservoirs. When the reservoir is compacted and densified, there is limited space for later dissolution, and therefore,

differential development of calcareous cementation leads to further densification of the reservoir. In summary, shale content, cuttings, and burial depth are the main factors that determine the density of deep low-permeability Gaoshangpu reservoirs. Calcareous cementation determines the middle and late diagenesis of the underwater distributary channel reservoir. The development of later dissolution has a significant effect on the improvement of underwater distributary channel reservoirs and is one of the important factors for favorable development of reservoirs. Calcareous cementation is more developed in mouth bar reservoirs in the early stages, resulting in the reservoir being densified at a depth of 3000 m, and the later-stage fluid erosion being weaker.

5 Conclusion

(1) In the sedimentary environment of the fan delta, factors such as rapid accumulation of sediments, high shale content, fine grain size, and medium sorting determine the weak compaction resistance of the deep low-permeability Gaoshangpu reservoir, which is the decisive factor for densification of the reservoir as the buried depth increases. Mechanical compaction and pressure solution lead to large porosity reduction and limited fluid dissolution in the later stage.

(2) The diagenetic evolution of the reservoir varies slightly under different sedimentary microfacies. Due to its relatively strong compaction resistance, the underwater distributary channel reservoir is significantly transformed by middle and late diagenesis. Dissolution is the main reason for reservoir improvement. During the middle stage of the diagenesis, the porosity was further reduced due to development of compaction, pre-solution, and cementation. At a depth of 3,000–4,000 m, compaction has a significant effect on reservoir permeability, which decreases by about 10 times, but the porosity does not reduce significantly.

(3) The sand body of the mouth bar is obviously influenced by sedimentation and diagenesis. Shale content, sorting, and particle size are decisive factors in the early diagenetic evolution. Strong compaction and calcareous cementation are the main reasons for densification of the reservoir at 3000 m, and delayed dissolution has a limited effect on reservoir reformation. The distal bar and sheet sand bar are most affected by sedimentation. In the early diagenesis stage, the reservoirs have been compacted and densified. However, the dissolution and transformation effect is very weak in the middle and late stages. The reservoir above 3000 m is of low permeability and ultra-low permeability.

(4) Feasible measures to efficiently exploit such reservoirs include volumetric fracturing at reservoirs with low

coordination numbers, communicating broadly developed dead pores, and improving connectivity.

(5) The study provides a geological basis for oilfield increase in reserves and production, as well as for efficient development of the Gaoshangpu reservoir, and meanwhile, provides a reference for evaluation of other low-permeability reservoirs in Nanpu Sag and similar areas that have the same geological conditions.

(6) The study provides a general reference for low-permeability reservoirs that are deposited in deltaic depositional settings.

Data availability statement

The original contributions presented in the study are included in the article/Supplementary Material; further inquiries can be directed to the corresponding author.

Author contributions

SW, XY, PS contributed in writing—review and editing, data curation, and writing—original draft preparation; YL, DL, LM, QW, LL and AR contributed in formal analysis, validation, and reviewing.

Conflicts of interest

YL is employed by CNOOC Research Institute Ltd., XY, DL, LM, QW, and LL are employed by Exploration and Development Research Institute, Jidong Oilfield Company, PetroChina.

The remaining authors declare that the research was conducted in the absence of any commercial or financial relationships that could be construed as a potential conflict of interest.

Publisher's note

All claims expressed in this article are solely those of the authors and do not necessarily represent those of their affiliated organizations, or those of the publisher, the editors, and the reviewers. Any product that may be evaluated in this article, or claim that may be made by its manufacturer, is not guaranteed or endorsed by the publisher.

References

Bjørlykke, K. (2014). Relationships between depositional environments, burial history and rock properties. Some principal aspects of diagenetic process in sedimentary basins. *Sediment. Geol.* 301, 1–14. doi:10.1016/j.sedgeo.2013.12.002

Fan, C. H., Li, H., Qin, Q. R., He, S., and Zhong, C. (2020a). Geological conditions and exploration potential of shale gas reservoir in Wufeng and Longmaxi Formation of southeastern Sichuan Basin, China. *J. Petroleum Sci. Eng.* 191, 107138. doi:10.1016/j.petrol.2020.107138

Fan, C. H., Li, H., Zhao, S. X., Qin, Q. R., Fan, Y., Wu, J. F., et al. (2020b). Formation stages and evolution patterns of structural fractures in marine shale: Case study of the lower silurian Longmaxi Formation in the changning area of the southern Sichuan basin, China. *Energy Fuel.* 34 (8), 9524–9539. doi:10.1021/acs.energyfuels.0c01748

Fan, C. H., Li, H., Qin, Q. R., Shang, L., Yuan, Y. F., and Li, Z. (2020c). Formation mechanisms and distribution of weathered volcanic reservoirs: A case study of the carboniferous volcanic rocks in northwest junggar basin, China. *Energy Sci. Eng.* 8, 2841–2858. doi:10.1002/ese3.702

Fan, C. H., Xie, H. B., Li, H., Zhao, S. X., Shi, X. C., Liu, J. F., et al. (2022). Complicated fault characterization and its influence on shale gas preservation in the southern margin of the Sichuan basin, China. *Lithosphere* 2022, 8035106. doi:10.2113/2022/8035106

Gao, Y., Zhang, J. L., Li, H. Y., and Yu, X. H. (2016). Diagenesis and porosity evolution of deep Es₃2+3 Formation in Gaoshangpu oilfield, Nanpu sag. *Fault-Block Oil Gas Field* 23 (06), 703–708. doi:10.6056/dkyqt201606005

Guo, X. S., Hu, D. F., Li, Y. P., Duan, J. B., Zhang, X. F., Fan, X. J., et al. (2019). Theoretical progress and key technologies of onshore ultra-deep oil/gas exploration. *Eng.* 5 (03), 458–470. doi:10.1016/j.eng.2019.01.012

He, P., Wang, Z. P., and Li, S. R. (2020). Diagenesis evolution of tight sandstone reservoirs in leping Formation of southern poyang depressio. *J. Hefei Univ. Technol. Sci.* 43 (08), 1122–1130. doi:10.3969/j.issn.1003-5060.2020.08.020

He, S., Li, H., Qin, Q. R., and Long, S. X. (2021). Influence of mineral compositions on shale pore development of Longmaxi Formation in the Dingshan area, southeastern Sichuan Basin, China. *Energy Fuel.* 35 (13), 10551–10561. doi:10.1021/acs.energyfuels.1c01026

He, S., Qin, Q. R., Li, H., and Zhao, S. X. (2022a). Geological characteristics of deep shale gas in the silurian Longmaxi Formation in the southern Sichuan basin, China. *Front. Earth Sci. (Lausanne)* 9, 818543. doi:10.3389/feart.2021.818155

He, S., Qin, Q. R., Li, H., and Wang, S. L. (2022b). Deformation differences in complex structural areas in the southern Sichuan basin and its influence on shale gas preservation: A case study of changning and luzhou areas. *Front. Earth Sci. (Lausanne)* 9, 818155. doi:10.3389/feart.2021.818534

Jiang, L. Z., Gu, J. Y., and Guo, B. C. (2004). Characteristics and mechanism of low permeability clastic reservoir in Chinese petroliferous basin. *Aata Pet. Sin.* 22 (01), 13–18. doi:10.14027/j.cnki.cjxb.2004.01.003

Karim, A., Pe-Piper, G., and Piper, D. J. (2010). Controls on diagenesis of lower cretaceous reservoir sandstones in the Western sable subbasin, offshore nova scotia. *Sediment. Geol.* 224 (1-4), 65–83. doi:10.1016/j.sedgeo.2009.12.010

Lai, J., Wang, G., Ran, Y., Zhou, Z., and Cui, Y. (2016). Impact of diagenesis on the reservoir quality of tight oil sandstones: The case of Upper Triassic Yanchang Formation Chang 7 oil layers in Ordos Basin, China. *J. Petrol Sci. Eng.* 145, 54–65. doi:10.1016/j.petrol.2016.03.009

Lai, J., Wang, G., Cai, C., Fan, Z., Wang, S., Chen, J., et al. (2018). Diagenesis and reservoir quality in tight gas sandstones: The fourth member of the upper triassic Xujiahe Formation, central Sichuan basin, southwest China. *Geol. J.* 53 (2), 629–646. doi:10.1002/gj.2917

Lan, C. L., Wang, J. G., Zhou, X. F., Dai, J. Y., Yang, M. H., and Cui, Z. Y. (2014). Impacts on sandstone reservoir quality of the third member of upper triassic yanchang formation, penyang oilfield of ordos basin, China. *Acta Petrol. Sin.* 30 (6), 1828–1840.

Law, B. E., and Dickinson, W. W. (1985). Conceptual model for origin of abnormally pressured gas accumulations in low-permeability reservoirs. *Am. Assoc. Pet. Geol. Bull.* 69 (8), 1295–1304. doi:10.1306/AD462BD7-16F7-11D7-8645000102C1865D

Li, H. (2022). Research progress on evaluation methods and factors influencing shale brittleness: A review. *Energy Rep.* 8, 4344–4358. doi:10.1016/j.egyr.2022.03.120

Li, C. L., Zhou, C. C., Li, X., Hu, F. L., Zhang, L., and Wang, W. J. (2010). A novel model for assessing the pore structure of tight sands and its application. *Appl. Geophys.* 7 (03), 283–291. doi:10.1007/s11770-010-0254-0

Li, H., Tang, H. M., Qin, Q. R., Fan, C. H., Han, S., Yang, C., et al. (2018a). Reservoir characteristics and hydrocarbon accumulation of Carboniferous volcanic weathered crust of Zhongguai high area in the Western Junggar Basin, China. *J. Cent. South Univ.* 25 (11), 2785–2801. doi:10.1007/s11771-018-3953-y

Li, J. J., Liu, Y., Gao, Y. J., Cheng, B. Y., Meng, F. L., and Xu, H. M. (2018b). Effects of microscopic pore structure heterogeneity on the distribution and morphology of remaining oil. *Petrol Explor. Dev.* 45 (06), 1112–1122. doi:10.1016/s1876-3804(18)30114-9

Li, Y., Shouli, X. U., Cai, L. I., Zhang, Y., Zhanjie, Z., and Peiyuan, Z. (2018c). Diagenesis-porosity evolution and "sweet spot" distribution of low permeability reservoirs: A case study from oligocene zhuhai Formation in wenchang A sag, pear river mouth basin, northern south China sea. *Petrol Explor. Dev.* 45 (2), 251–263. doi:10.1016/s1876-3804(18)30028-4

Li, H., Tang, H. M., and Zheng, M. J. (2019a). Micropore structural heterogeneity of siliceous shale reservoir of the Longmaxi Formation in the southern Sichuan Basin, China. *Minerals* 9, 548. doi:10.3390/min9090548

Li, H., Tang, H. M., Qin, Q. R., Wang, Q., and Zhong, C. (2019b). Effectiveness evaluation of natural fractures in Xujiahe Formation of Yuanba area, Sichuan basin, China. *Arab. J. Geosci.* 12 (6), 194. doi:10.1007/s12517-019-4292-5

Li, H., Tang, H. M., Qin, Q. R., Zhou, J. L., Qin, Z. J., Fan, C. H., et al. (2019c). Characteristics, formation periods and genetic mechanisms of tectonic fractures in the tight gas sandstones reservoir: A case study of Xujiahe Formation in YB area, Sichuan basin, China. *J. Petrol Sci. Eng.* 178, 723–735. doi:10.1016/j.petrol.2019.04.007

Li, H., Qin, Q. R., Zhang, B. J., Ge, X. Y., Hu, X., Fan, C. H., et al. (2020). Tectonic fracture formation and distribution in ultradeep marine carbonate gas reservoirs: A case study of the maokou Formation in the jiulongshan gas field, Sichuan basin, southwest China. *Energy Fuel.* 34 (11), 14132–14146. doi:10.1021/acs.energyfuels.0c03327

Li, H., Wang, Q., Qin, Q. R., and Ge, X. Y. (2021a). Characteristics of natural fractures in an ultradeep marine carbonate gas reservoir and their impact on the reservoir: A case study of the maokou Formation of the jls structure in the Sichuan basin, China. *Energy Fuel.* 35 (16), 13098–13108. doi:10.1021/acs.energyfuels.1c01581

Li, K., Xi, K. L., Cao, Y. C., Niu, X. B., Wu, S. T., Feng, S. B., et al. (2021b). Chlorite authigenesis and its impact on reservoir quality in tight sandstone reservoirs of the Triassic Yanchang formation, southwestern Ordos basin, China. *J. Petrol Sci. Eng.* 205, 108843. doi:10.1016/j.petrol.2021.108843

Li, J., Qin, Q. R., Li, H., and Wan, Y. F. (2022a). Numerical simulation of the stress field and fault sealing of complex fault combinations in Changning area, Southern Sichuan Basin, China. *Energy Sci. Eng.* 10, 278–291. doi:10.1002/ese3.1044

Li, J., Li, H., Yang, C., Wu, Y. J., Gao, Z., and Jiang, S. L. (2022b). Geological characteristics and controlling factors of deep shale gas enrichment of the Wufeng-Longmaxi Formation in the southern Sichuan Basin, China. *Lithosphere* 2022, 4737801. doi:10.2113/2022/4737801

Li, H., Zhou, J. L., Mou, X. Y., Guo, H. Z., Wang, X. X., An, H. Y., et al. (2022c). Pore structure and fractal characteristics of the marine shale of the Longmaxi Formation in the Changning Area, Southern Sichuan Basin, China. *Front. Earth Sci.* 10, 1018274. doi:10.3389/feart.2022.1018274

Liu, L., Sun, Y. H., Chen, C., Lou, R., and Wang, Q. (2022). Fault reactivation in No.4 structural zone and its control on oil and gas accumulation in Nanpu sag, Bohai Bay Basin, China. *Petrol Explor. Dev.* 49 (04), 824–836. doi:10.1016/s1876-3804(22)60313-6

Mingjie, L. I. U., Zhen, L. I. U., Jingjing, L. I. U., Wenqi, Z. H. U., Huang, Y., and Xing, Y. (2014). Coupling relationship between sandstone reservoir densification and hydrocarbon accumulation: A case from the yanchang Formation of the xifeng and ansai areas, ordos basin. *Petrol Explor. Dev.* 41 (2), 185–192. doi:10.1016/S1876-3804(14)60021-5

Ren, D., Zhou, D., Liu, D., Dong, F., Ma, S., and Huang, H. (2019). formation mechanism of the upper triassic yanchang formation tight sandstone reservoir in ordos basin—take chang 6 reservoir in jiyuan oil field as an example. *J. Petrol Sci. Eng.* 178, 497–505. doi:10.1016/j.petrol.2019.03.021

Shanley, K. W., Cluff, R. M., and Robinson, J. W. (2004). Factors controlling prolific gas production from low-permeability sandstone reservoirs: Implications for resource assessment, prospect development, and risk analysis. *Am. Assoc. Pet. Geol. Bull.* 88 (8), 1083–1121. doi:10.1306/03250403051

Wang, Y., and Chen, S. Y. (2016). Meandering river sand body architecture and heterogeneity: A case study of permian meandering river outcrop in palougou, baode, shanxi province:A case study of permian meandering river outcrop in palougou, baode, shanxi province. *Petrol Explor. Dev.* 43 (02), 230–240. doi:10.1016/S1876-3804(16)30026-X

Wang, Y. J., Song, X. M., and Gu, F. (2010). Sedimentary character and sand body structure in second and third sub-formation of Sha3 formation, north deep reservoir of Gaoshangpu oilfield. *Petroleum Geol. Recovery Effic.* 17 (2), 14–16. doi:10.13673/j.cnki.cn37-1359/te.2010.02.014

Wang, Y. L., Shao, G. C., Liu, J., and Fan, G. F. (2013). Reservoir characteristics research and evaluation classification of Maxi Sha-3 formation of Huabei oilfield. *Petroleum Reserv. Eval. Dev.* 3 (06), 1–4. doi:10.13809/j.cnki.cn32-1825/te.2013.06.001

Wang, S. L., Li, H., Lin, L. F., and Yin, S. (2022). Development characteristics and finite element simulation of fractures in tight oil sandstone reservoirs of Yanchang Formation in Western Ordos Basin. *Front. Earth Sci.* 9, 823855. doi:10.3389/feart.2021.823855

Wu, J., Liu, Z. G., Zhu, C., Gong, Q. S., Xia, Z. Y., Song, G. Y., et al. (2020). Characteristics of deep tight sandstone reservoirs and their controlling factors in the Middle-Lower Jurassic in the Yiqikelike area, Kuqa depression. *China Pet. Explor.* 25 (06), 58–67. doi:10.3969/j.issn.1672-7703.2020.06.006

Xi, K., Cao, Y., Jahren, J., Zhu, R., Bjørlykke, K., Haile, B. G., et al. (2015). Diagenesis and reservoir quality of the lower cretaceous quantou formation tight sandstones in the southern songliao basin, China. *Sediment. Geol.* 330, 90–107. doi:10.1016/j.sedgeo.2015.10.007

Xie, J., Hu, W. S., Chen, S. Y., Yu, S. B., and Chen, P. P. (2017). Reservoir architectural analysis of the braided fluvial delta of the lower oil layer in the 1st block of Tahe Oilfield[J]. *Petroleum Geol. Recovery Effic.* 24 (05), 46–52. doi:10.13673/j.cnki.cn37-1359/te.2017.05.007

Xu, K., Dai, J. S., Feng, J. W., Wang, B. F., ShangFang, L., Wang, S., et al. (2020). Predicting 3D heterogeneous *in situ* stress field of Gaoshangpu oilfield northern area, Nanpu sag, Bohai bay basin, China. *Arab. J. Geosci.* 13 (1), 43–15. doi:10.1007/s12517-019-5043-3

Yang, X. L., Dong, X. H., and Guo, A. H. (2016a). Sedimentary environment and reservoir characteristics during depositional stage of Es3 in Gaobei ramp region. *Lithol. Reserv.* 28 (01), 65–71. doi:10.3969/j.issn.1673-8926.2016.01.008

Yang, Z., He, S., Guo, X., Li, Q., Chen, Z., and Zhao, Y. (2016b). Formation of low permeability reservoirs and gas accumulation process in the daniudi gas field, northeast ordos basin, China. *Mar. Petrol Geol.* 70, 222–236. doi:10.1016/j.marpetgeo.2015.10.021

Zeng, L., Jiang, J., and Yang, Y. (2010). Fractures in the low porosity and ultra-low permeability glutenite reservoirs: A case study of the late eocene hetaoyuan Formation in the anpeng oilfield, nanxiang basin, China. *Mar. Petrol Geol.* 27 (7), 1642–1650. doi:10.1016/j.marpetgeo.2010.03.009

Zhu, R. K., Zhou, C. N., Zhang, X., He, W. B., and Wang, Z. F. (2009). Characteristics and formation mechanism of low porosity-low permeability reservoirs of the Triassic Xujiahe Formation in Jiannan area, eastern Sichuan Basin. *Sci. Sin.* 39 (03), 327–339. doi:10.7605/gdlxb.2014.01.009

ZinsaloJoël, M., Louis, L., and Raymond, J. (2021). Sustainable electricity generation from an Enhanced Geothermal System considering reservoir heterogeneity and water losses with a discrete fractures model. *Appl. Therm. Eng.* 192, 116886. doi:10.1016/j.applthermaleng.2021.116886

Zou, C., Zhu, R., Liu, K., Su, L., Bai, B., Zhang, X., et al. (2012). Tight gas sandstone reservoirs in China: Characteristics and recognition criteria. *J. Petrol Sci. Eng.* 88, 82–91. doi:10.1016/j.petrol.2012.02.001